Nucleation and growth kinetics of spiral steps on TiN(111): An *in situ* low-energy electron microscopy study

S. Kodambaka[a)] and J. Bareño
Frederick Seitz Materials Research Laboratory and the Department of Materials Science,
University of Illinois, 104 South Goodwin Avenue, Urbana, Illinois 61801

S. V. Khare
Department of Physics and Astronomy, The University of Toledo, 2801 West Bancroft Street,
Toledo, Ohio 43606

W. Święch, I. Petrov, and J. E. Greene
Frederick Seitz Materials Research Laboratory and the Department of Materials Science,
University of Illinois, 104 South Goodwin Avenue, Urbana, Illinois 61801

We use *in situ* low-energy electron microscopy to investigate the near-equilibrium dynamics of TiN(111) steps, pinned by surface-terminated dislocations, as a function of N_2 pressure p_{N_2} and time during annealing of TiN(111) layers at temperatures T between 1600 and 1735 K. At each T, we observe the nucleation and growth of spiral steps rotating around dislocation cores. The spirals undergo a shape-preserving motion with a constant angular velocity ω as they grow inward, normal to the surface, forming vacancy pits. We find that ω for successive spirals emanating from the same source decreases slowly with time at all p_{N_2} values between vacuum and 5×10^{-7} Torr. From the $\omega(T)$ data, we obtain an activation energy of 4.6 ± 0.2 eV, irrespective of p_{N_2}, for the growth of spiral steps. © *2005 American Institute of Physics*. [DOI: 10.1063/1.1977193]

I. INTRODUCTION

Dislocations terminating on surfaces can strongly influence nanostructure stability, mechanical properties of thin films, chemical reactions, transport phenomena, and other surface processes. However, since most theoretical and experimental studies have focused on step formation due to dislocations at surfaces during crystal growth[1–7] or etching by evaporation,[8,9] very little is known concerning the near-equilibrium dynamics of dislocations at surfaces.

Recently, the observation of a thermally driven nucleation and growth process for spiral steps around cores of dislocations terminating on TiN(111) was reported.[10] This process, leading to dislocation-mediated surface roughening, occurs at elevated temperatures in the absence of applied external stress and net mass change and is both qualitatively and quantitatively different from step-curvature-driven island dynamics[11] and Burton-Cabrera-Frank (BCF) spiral growth.[1] While the phenomenon of two-dimensional (2D) TiN(111) island decay occurs due to surface mass transport across highly permeable steps in the detachment-limited regime,[12] the details of the dominant mass transport mechanism governing TiN(111) spiral growth kinetics are still not understood.

The results of previous low-energy electron microscopy (LEEM) studies[10] suggest that dislocation-induced bulk point-defect migration leads to TiN(111) spiral step formation. This is plausible since TiN is known to have a wide phase field and can sustain high concentrations of both anion and cation vacancies[13] which can migrate between the bulk and the surface. In the case of TiO_2, varying the O_2 pressure leads to a change in the bulk Ti concentration resulting in surface step motion.[14–17] Here, we focus on the effects of N_2 pressure p_{N_2} on the nucleation and growth kinetics of spiral steps on TiN(111) in order to gain insight into mass transport mechanisms controlling TiN(111) spiral step kinetics.

In this paper, we present the results of *in situ* LEEM (Ref. 18) studies of the near-equilibrium dynamics of surface-terminated dislocations during annealing of atomically smooth TiN(111) layers at temperatures T between 1600 and 1735 K as a function of annealing time t and p_{N_2}. At each T, we observe (1) the decay of 2D TiN(111) adatom islands and (2) the nucleation and growth of $\langle 110 \rangle$-oriented TiN(111) spiral steps rotating around dislocation cores. The spirals undergo a shape-preserving motion with a constant angular velocity ω as they grow inward, normal to the surface. However, ω for successive spirals emanating from the same source decreases with time, irrespective of p_{N_2}.

II. EXPERIMENTAL PROCEDURE

Epitaxial TiN(111) layers, 1500 Å thick, are grown on polished Al_2O_3(0001) substrates (0.5 mm thick × 9-mm diameter, miscut < 0.1°) at $T_s = 1050$ K in a load-locked multichamber ultrahigh-vacuum (UHV) system using magnetically unbalanced dc magnetron sputter deposition[19] following the procedure described in Ref. 20. Prior to deposition, the substrates are annealed in air at 1673 K for 4 h to obtain large step-free terraces. Then, the back sides of the substrates are coated with 1-μm-thick TiN layers to avoid substrate decomposition during electron-beam heating. The TiN(111) samples are annealed *in situ* in the magnetron deposition

a)Electronic mail: kodambaka@mrl.uiuc.edu

98, 034901-1

system for $\simeq 21$ h at $T=1273$–1500 K in 1.0–5.0 mTorr of N_2. This deposition and annealing procedure is carried out three times in succession in order to obtain smooth surfaces. The samples are then transferred to an UHV multichamber LEEM system[21] with a base pressure of 2×10^{-10} Torr.

The LEEM preparation chamber is equipped with facilities for residual gas analysis (RGA), electron-beam evaporation, ion sputtering, Auger electron spectroscopy (AES), and low-energy electron diffraction (LEED). Sample temperatures are measured by optical pyrometry and calibrated using temperature-dependent TiN emissivity data obtained by spectroscopic ellipsometry. The TiN layers are degassed in the sample preparation chamber at 1073 K for approximately 2 h. This procedure results in sharp 1×1 LEED patterns with a threefold symmetry, corresponding to an in-plane atomic spacing of 2.99 Å, as expected for bulk-terminated TiN(111).[20] *In situ* AES analyses indicate that the samples contain $\simeq 2$ mole % oxygen, most likely in the form of TiO which is isostructural[22] and mutually soluble with TiN.

Homoepitaxial TiN(111) overlayers, 50–200 Å thick, are deposited in the LEEM system at 1023 K by reactive evaporation from Ti rods (99.999% purity) at a rate of $\simeq 0.02$ ML/s. The samples are then annealed for >5 h in 5×10^{-8}-Torr N_2 (99.999%) at temperatures $T>1200$ K. This procedure results in TiN(111) terraces containing three-dimensional (3D) mounds, consisting of stacks of 2D TiN adatom islands, in defect-free areas as well as spiral structures in the presence of surface-terminated dislocations.

Bright-field (BF) LEEM images of the decay of 2D islands and the growth of spiral steps are acquired at a video rate of 30 frames/s as a function of annealing time t, N_2 pressure p_{N_2}, and temperature T. Pixel resolution in a 5.6-μm field of view is $\simeq 118$ Å. Typical electron-beam energies are 5–25 eV. The samples are allowed to thermally stabilize at each temperature for 10–15 s prior to acquiring LEEM videos. From each measurement sequence, time-dependent island areas A and spiral step boundary coordinates $r(\theta,t)$ are obtained using IMAGE SXM, an image processing software.[23] Since the angular velocity ω is a constant proportional to the growth rate, $(1/2)\int_{\theta_1}^{\theta_2}\{d[r(\theta,t)]^2/dt\}d\theta$, for an outwardly moving spiral step segment far from the core,[24] we measure ω as a function of time and temperature. LEEM images of a given spiral acquired at times t_n ($n=1,2,\ldots,m$) are superposed in order to obtain the spiral period τ and, hence, the frequency ω ($=2\pi/\tau$). ω values for all spirals, irrespective of p_{N_2} and T, are found to be equal, within experimental uncertainties of 3%, to spiral frequencies calculated by fitting a function of the form $r(\theta,t)=a(\theta)(\theta+\omega t)$ to the spiral step boundary coordinates $r(\theta,t)$. Since TiN(111) spirals exhibit threefold symmetry, we use $a(\theta)=a_0[1+a_1\sin(3\theta+a_2)]$ in which a_0, a_1, and a_2 are time-independent fitting parameters.

III. RESULTS AND DISCUSSION

Figures 1(a)–1(d) are representative BF LEEM images (5.6-μm fields of view) obtained from a TiN(111) sample during annealing at $T=1670$ K with $p_{N_2}=5\times10^{-8}$ Torr. The images, part of a 30 frame/s video file, were acquired at
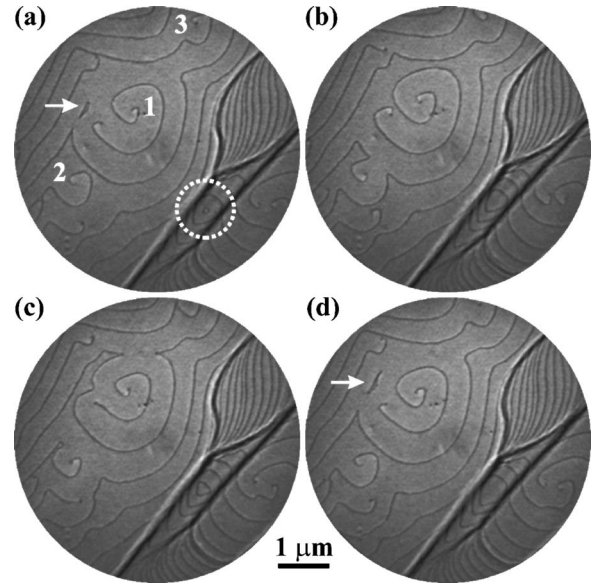
FIG. 1. (a)–(d): Representative BF-LEEM images (field of view=5.6 μm) of a TiN(111) sample during annealing at $T=1670$ K in N_2 at a pressure of $p_{N_2}=5\times10^{-8}$ Torr for times t of (a) 0, (b) 60, (c) 120, and (d) 180 s.

times $t=0$, 60, 120, and 180 s. (We define $t=0$ as the time at which the first image is acquired.) Figure 1 illustrates both the dissolution of 2D TiN(111) adatom islands on top of mound structures [see the highlighted circular region in Fig. 1(a)] and the nucleation and growth of TiN(111) spiral steps at the cores of three surface-terminated dislocations [labeled 1, 2, and 3 in Fig. 1(a)]. We also observe dissolution of nonequilibrium shaped 2D islands, identified by the arrows in Figs. 1(a) and 1(d), that form due to the oppositely directed motion of neighboring terrace steps.

The total step length of spirals increases while rotating around their respective dislocation cores with an angular velocity ω. For example, the spiral labeled 1 in Fig. 1(a) undergoes one complete rotation within $\simeq 180$ s at $T=1670$ K and becomes geometrically identical to the one shown in Fig. 1(d). That is, the spiral step motion is periodic with time τ and frequency ω. During the period τ, the dislocation core moves by a unit step height, $a_\perp=2.4$ Å, normal into the surface. That is, the observed spiral step motion results in the formation of pits, analogous to those observed during etching. This process is cumulative and the depth of the spiral structures increases with annealing time although at an ever decreasing rate (see Fig. 3). In the case of a few spirals, however, spiral step motion terminates due either to the motion of the dislocation core or annihilation of the dislocation with another oppositely signed dislocation. Note that the observed step growth during annealing in the absence of net mass gain or loss[25] is a localized process which occurs only at the dislocation cores. This is in contrast with the growth spirals described by the BCF theory,[1] for which the growth flux is nonlocalized resulting in spirals with curvature-dependent step velocities and whose areas increase nonlinearly with time.[1]

Figure 2(a) contains typical plots of the area A of a 2D island and the angular rotation ωt traversed by a spiral as a function of annealing time t at $T=1670$ K with $p_{N_2}=5$
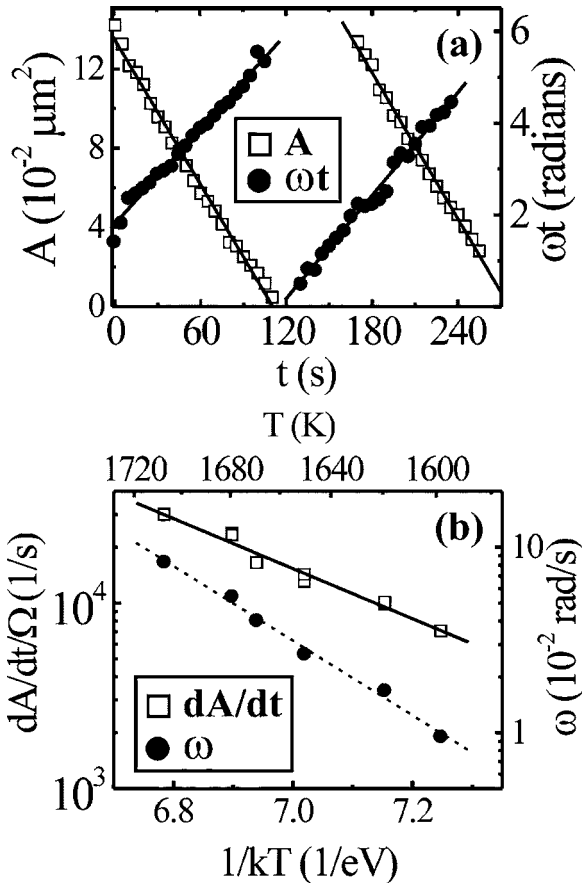
FIG. 2. (a) Typical plots of area A of island (open squares) and angular rotation ωt traversed by a spiral (solid circles) vs annealing time t at T $=1670$ K with $p_{N_2}=5\times10^{-8}$ Torr. The symbols in (a) are the measured data for 2D TiN(111) islands in the highlighted region and spirals labeled 1 in Fig. 1(a), while the solid lines are fits obtained using linear least-squares analyses. (b) Plots of 2D TiN(111) island decay rates dA/dt (open squares) and spiral angular frequencies ω (solid circles) vs annealing temperature T. The solid and dashed lines are linear least-squares fits to the data.

FIG. 3. ω vs t plot for successive spiral steps in the region highlighted in the associated LEEM image (field of view=5.6 μm). The data were acquired during annealing a TiN(111) sample at $T=1727$ K with $p_{N_2}=5\times10^{-8}$ Torr. The dashed line is a linear least-squares fit to the measured data.

$\times10^{-8}$ Torr. The symbols in Fig. 2(a) correspond to the measured data while the solid lines are fitted using least-squares analyses. These two double data sets correspond to the successive decay of two adjacent islands on the highlighted mound in Fig. 1(a) and the growth of two successive spirals around the dislocation labeled 1 in Fig. 1(a). We have measured the decay rates dA/dt for 26 2D adatom islands and the generation frequencies ω for 64 spirals at temperatures T $=1600-1735$ K and N_2 pressures $p_{N_2}\simeq0-5\times10^{-7}$ Torr. We find that all island areas decrease linearly with time at a temperature-dependent constant rate while all spirals grow with an angular velocity ω. For example, dA/dt $=(12.2\pm0.2)\times10^{-4}$ $\mu m^2/s$ and $\omega=(3.6\pm0.1)$ $\times10^{-2}$ rad/s$[\tau=175\pm5$ s$]$ at $T=1670$ K.

The temperature dependences of dA/dt and ω are shown in Fig. 2(b) for data acquired at $p_{N_2}=5\times10^{-8}$ Torr. From linear least-squares analyses of the data, we obtain an activation energy E_{spiral} of 4.6 ± 0.2 eV with a prefactor of $10^{12.6\pm0.6}$ s^{-1} for the growth of TiN(111) spirals and an activation energy E_{island} of 3.1 ± 0.2 eV with a prefactor of $10^{13.6\pm0.6}$ s^{-1} for the decay of 2D TiN(111) islands. E_{spiral} is the total energy required for point-defect formation and migration along the dislocation (also referred to as "pipe

diffusion").[26,27] This is physically reasonable since bulk point-defect migration has a smaller activation barrier along dislocation lines than in dislocation-free areas. The measured activation energies E_{spiral} and E_{island} are consistent with previous results[10,12] determined from LEEM data acquired during annealing a TiN(111) sample at a constant N_2 pressure $p_{N_2}=5\times10^{-8}$ Torr and hence provide the basis for carrying out additional experiments over extended annealing times while varying p_{N_2}.

First, we studied the long-time behavior of spiral growth rates. Figure 3 is a typical plot of ω vs t values (solid circles) obtained from 17 successive spirals generated from the same dislocation core (highlighted in the associated LEEM image) while annealing a TiN(111) sample at $T=1727$ K with p_{N_2} held constant at 5×10^{-8} Torr. We find that ω decreases monotonically from $\simeq0.09$ to $\simeq0.07$ rad/s, i.e., an $\simeq22\%$ reduction in ω, within 1340 s at 1727 K. If we assume a linear relationship, the $\omega(t)$ data can be fit using least-squares analyses (dashed line in Fig. 3). The observed decrease in ω with time can be attributed to (1) the effect of already existing steps on the nucleation of new steps (a "back-force" effect[28]) and/or (2) equilibration of the point-defect concentration in the bulk. In the first case, the geometry of the spiral structures, while in the second case, the N_2 pressure, could affect the TiN(111) spiral step growth kinetics. Since the spirals in our experiments are situated in very similar surface geometries, the effect of local environment on spiral growth kinetics cannot be determined. Thus, we focused on the effects of p_{N_2}.

We measured ω while varying p_{N_2} between zero and 5 $\times10^{-7}$ Torr at a constant annealing temperature. Figure 4 contains typical plots of ω (solid circles) and dA/dt (open squares) as a function of annealing time t. The data are obtained from LEEM images of the spiral labeled 1 and the 2D TiN(111) islands highlighted in Fig. 1 during annealing at $T=1670$ K. p_{N_2}, set initially to 5×10^{-8} Torr, is suddenly reduced to zero ($\leqslant5\times10^{-9}$ Torr) at $t=390$ s and then varied between zero and 5×10^{-7} Torr. ω and dA/dt, while exhibiting an overall decrease with time, do not vary systematically with p_{N_2}.

Temperature-dependent ω measurements for spirals are shown in Fig. 5. The solid symbols represent $\omega(T)$ data acquired for spirals generating at a given source during annealing in 5×10^{-8}-Torr N_2 over a period of 3240 s. The open
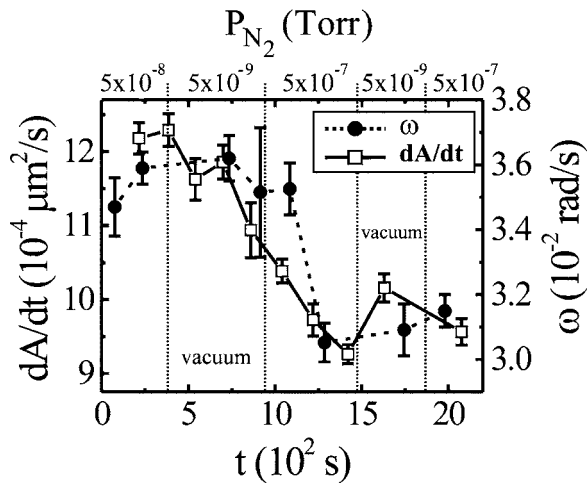
FIG. 4. Plots of dA/dt (open squares) and ω (solid circles) vs t for 2D TiN(111) islands in the highlighted region of Fig. 1(a) and spirals labeled 1 in Fig. 1(a). The data were acquired during annealing a TiN(111) sample at $T=1670$ K while varying p_{N_2} between zero and 5×10^{-7} Torr as shown.

symbols are $\omega(T)$ data for spirals originating at the same source during subsequent annealing in vacuum. These data were obtained in 2520 s and the time interval between the two sets of measurements is 5040 s. Using least-squares analyses, we obtain $E_{spiral}=4.5\pm0.4$ eV with a prefactor of $10^{12\pm1.3}$ s^{-1} for spiral growth at $p_{N_2}=5\times10^{-8}$ Torr and $E_{spiral}=4.6\pm0.1$ eV with a prefactor of $10^{12.0\pm0.3}$ s^{-1} for spiral growth in vacuum. The fact that we obtain similar E_{spiral} values, irrespective of the N$_2$ pressure, provides further evidence that the TiN(111) spiral step growth kinetics are not strongly influenced by p_{N_2}. Thus, our results suggest that molecular N$_2$ does not significantly change the surface and bulk compositions of N-terminated TiN(111). However, this does not rule out the effects of atomic N on the spiral step growth kinetics, which requires further investigation.
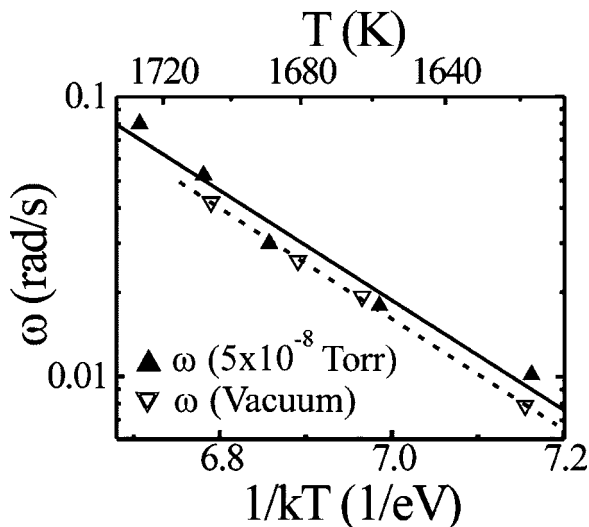
FIG. 5. Plots of ω vs annealing temperature T for TiN(111) spirals during annealing in 5×10^{-8}-Torr N$_2$ (solid symbols) and in vacuum (open symbols). The solid and dashed lines are linear least-squares fits to the data and correspond to activation energies E_{spiral} of 4.5±0.4 and 4.6±0.1 eV for spiral step motion in 5×10^{-8}-Torr N$_2$ and vacuum ($\leqslant5\times10^{-9}$), respectively.

IV. SUMMARY

We use *in situ* low-energy electron microscopy to investigate the near-equilibrium dynamics of surface-terminated dislocations during annealing of atomically smooth TiN(111) layers at temperatures between 1600 and 1735 K in the absence of applied external stress or net mass change. At each temperature, we observe the nucleation and growth of spiral steps rotating with a constant angular frequency ω around dislocation cores. However, the angular frequency of successive spirals emanating from the same source decreases with annealing time at all N$_2$ pressures between vacuum and 5×10^{-7} Torr. From the $\omega(T)$ data, we obtain a constant activation energy of 4.6±0.2 eV for the growth of spiral steps irrespective of N$_2$ pressure. These results demonstrate that TiN(111) spiral step growth kinetics are not strongly influenced by the N$_2$ pressure.

[1] W. K. Burton, N. Cabrera, and F. C. Frank, Philos. Trans. R. Soc. London, Ser. A **243**, 299 (1951).
[2] A. R. Verma and S. Amelinckx, Nature (London) **167**, 939 (1951).
[3] I. S. Aranson, A. R. Bishop, I. Daruka, and V. M. Vinokur, Phys. Rev. Lett. **80**, 1770 (1998).
[4] A. Karma and M. Plapp, Phys. Rev. Lett. **81**, 4444 (1998).
[5] H. H. Teng, P. M. Dove, C. A. Orme, and J. J. De Yoreo, Science **282**, 724 (1998).
[6] C. M. Pina, U. Becker, P. Risthaus, D. Bosbach, and A. Putnis, Nature (London) **395**, 483 (1998).
[7] Y. Cui and L. Li, Phys. Rev. B **66**, 155330 (2002).
[8] N. Cabrera and M. M. Levine, Philos. Mag. **1**, 450 (1956).
[9] T. Surek, G. M. Pound, and J. P. Hirth, Surf. Sci. **41**, 77 (1974).
[10] S. Kodambaka, S. V. Khare, W. Święch, K. Ohmori, I. Petrov, and J. E. Greene, Nature (London) **429**, 49 (2004).
[11] M. Zinke-Allmang, L. C. Feldman, and M. H. Grabow, Surf. Sci. Rep. **16**, 377 (1992).
[12] S. Kodambaka, N. Israeli, J. Bareño, W. Święch, K. Ohmori, I. Petrov, and J. E. Greene, Surf. Sci. **560**, 53 (2004).
[13] J.-E. Sundgren, B. O. Johansson, A. Rockett, S. A. Barnett, and J. E. Greene, in *Physics and Chemistry of Protective Coatings*, edited by J. E. Greene, W. D. Sproul, and J. A. Thornton, AIP Conf. Proc. No. 149 (American Institute of Physics, New York, 1986).
[14] K. F. McCarty and N. C. Bartelt, Phys. Rev. Lett. **90**, 046104 (2003).
[15] K. F. McCarty and N. C. Bartelt, Surf. Sci. **540**, 157 (2003).
[16] K. F. McCarty and N. C. Bartelt, Surf. Sci. **527**, L203 (2003).
[17] K. F. McCarty and N. C. Bartelt, J. Cryst. Growth **270**, 691 (2004).
[18] E. Bauer, Rep. Prog. Phys. **57**, 895 (1994).
[19] I. Petrov, F. Adibi, J. E. Greene, W. D. Sproul, and W.-D. Münz, J. Vac. Sci. Technol. A **10**, 3283 (1992).
[20] S. Kodambaka, S. V. Khare, V. Petrova, D. D. Johnson, I. Petrov, and J. E. Greene, Phys. Rev. B **67**, 035409 (2003).
[21] R. M. Tromp and M. C. Reuter, Ultramicroscopy **36**, 99 (1991).
[22] Inorganic Index to Powder Diffraction File, Card Nos. 38-1420 and 08-0117, Joint Committee on Powder Diffraction Standards, Pennsylvania, 1997 (unpublished), for TiN and TiO, respectively.
[23] S. Barrett, IMAGE SXM, developed by Prof. Steve Barrett, Surface Science Research Centre, Liverpool, England, 2002; http://reg.ssci.liv.ac.uk
[24] The growth rates of spiral steps with high curvatures ($>2\times10^{-4}$ Å^{-1}) near

the core are nonlinear. Hence, we only measure areas of spirals corresponding to linear growth rates with $\theta_1 = \pi$ and $\theta_2 = 3\pi$.

[25] We have ruled out evaporation, at annealing temperatures $T \simeq 0.5 T_m$, where $T_m = 3200$ K is the melting point. This conclusion was based upon the fact that the calculated values for cohesive energy of TiN ($\simeq 14$ eV) and desorption energies for TiN (8.8 eV) and Ti (10 eV) adspecies from N-terminated TiN(111) [D. Gall, S. Kodambaka, M. A. Wall, I. Petrov, and J. E. Greene, J. Appl. Phys. **93**, 9086 (2003)] are significantly higher than the measured activation energy of 4.6±0.2 eV for spiral growth.

[26] V. L. Indenbom and Z. K. Saralidze, in *Elastic Strain Fields and Dislocation Mobility*, edited by V. L. Indenbom and J. Lothe (Elsevier Science, Amsterdam, 1992).

[27] R. C. Picu and D. Zhang, Acta Mater. **52**, 161 (2004).

[28] T. Surek, J. P. Hirth, and G. M. Pound, J. Cryst. Growth **18**, 20 (1973).